Polymer Testing 100 (2021) 107267

Contents lists available at ScienceDirect

Polymer Testing

journal homepage: www.elsevier.com/locate/polytest

Quantifying damping coefficient and attenuation at different frequencies for graphene modified polyurethane by drop ball test

Arash Dashtkar, MSc [a], Homayoun Hadavinia [a,*], Jose Barros-Rodriguez, PhD [a], Neil A. Williams, PhD [b], Matthew Turner, PhD [c], Samireh Vahid, PhD [a]

[a] School of Engineering & Environment, Kingston University London, UK
[b] School of Life Sciences, Pharmacy and Chemistry, Kingston University London, UK
[c] Hive Composites Ltd, Loughborough, England, UK

ARTICLE INFO

Keywords:
Polyurethane
Graphene
Damping property
Attenuation
Wind turbine blade coating

ABSTRACT

In this study, polyurethane (PU) was modified by direct mixing of carboxyl functionalised graphene (GNP–COOH) referred to as f-GNP, without using any solvent, during in-situ polymerization. In a further attempt, the neat PU was modified with f-GNP and a hydrophobic silica-based solution (SG) during in-situ polymerization. The damping coefficient and attenuation capacity of neat polyurethane (PU), f-GNP based PU nanocomposite (PU + f-GNP), and f-GNP and hydrophobic silica-based solution PU nanocomposite (PU + f-GNP + SG), together with polytetrafluoroethylene (PTFE), high-density polyethylene (HDPE), ultra-high molecular weight polyethylene (UHMWPE), polyethylene terephthalate (PET), polyvinyl chloride (PVC) and NYLON have been obtained by the drop ball tests under controlled and consistent conditions. The results show that among the tested materials, polyurethane modified with carboxyl functionalised graphene and silica-based Sol-Gel (PU + f-GNP + SG) displays the greatest attenuations and PTFE the least.

The attenuation of the various materials has been identified with the SVD-QR method. This experimental modal analysis method has been used to analyse the free response signal of the system during the drop ball test and identify the modal parameters such as damping ratio and frequency of the modes of deformation of the system. The drop ball test results show that the damping coefficient of polyurethane modified with 0.5 wt% carboxyl functionalised graphene (PU + f-GNP) increased by 37% at frequency range 200–300 Hz, by 34% at frequency range 500–600 Hz and by 32% at frequency range 700–1000 Hz. The developed nanocomposite materials have great potential for protecting leading edge erosion (LEE) of wind turbine.

1. Introduction

Polymers are one of the materials that used for energy absorption and vibration damping in many devices [1] because they have better attenuation capability than other materials such as metals and ceramics.

The viscoelastic behaviour of polymers is a key reason why they are used for application such as energy absorption and vibration damping. In viscoelastic materials, the elastic elements store energy during deformation and release it in the process of strain recovery [2]. During unloading, some of the energy is recovered with the rest being dissipated in the form of heat. Another property of a vibration damping material is attenuation which can happen through two mechanisms: absorption and scattering of energy. In absorption, wave energy [3] is converted to heat by the elastic motion of particles; in other words, materials stores energy when they are elastically loaded and when unloaded, some of the mechanical energy is lost and dissipated as heat. Scattering is a result of inhomogeneity in a material such as crystal discontinuities, grain boundaries, inclusions, particles and voids [3]. Scattering causes the energy of the coherent, collimated waves to be converted into incoherent, divergent waves through reflection and refraction [2].

Polyurethane (PU) elastomers is a polymer, which contains the urethane group –NH–CO–O–; this group is formed by a combination of hard (isocyanate) and elastic (polyol) parts, and changing these components creates a range of characteristics for various polyurethane elastomers. Polyurethane elastomers are superior in resistance to abrasion, oxidation, tear, and chemicals (oil, gas). They are also transparent,

* Corresponding author.
E-mail addresses: k1547266@kingston.ac.uk (A. Dashtkar), h.hadavinia@kingston.ac.uk (H. Hadavinia), j.barrosrodriguez@kingston.ac.uk (J. Barros-Rodriguez), n.a.williams@kingston.ac.uk (N.A. Williams), m.turner@hivecomposites.com (M. Turner), s.vahid@kingston.ac.uk (S. Vahid).

https://doi.org/10.1016/j.polymertesting.2021.107267
Received 9 February 2021; Accepted 5 June 2021
Available online 9 June 2021

have good adhesion and are used for vibration-damping applications [4]. The loss angle δ is the phase shift between stress and strain. An equivalent measure for material loss factor (η) is the loss tangent, defined as $\tan\delta = \eta = \frac{G''}{G'}$, where G' is the storage modulus and G'' is the loss modulus. The loss factor is a measure of the energy dissipation capability of the material. It is realized that by adding inorganic fillers to polyurethane, the $\tan\delta$ increases significantly. For example, adding 10% silica increases the maximum $\tan\delta$ value of Polyurethane/Poly-ethyl-methacrylate interpenetrating network (PU/PEMA IPNs) from 0.44 to 0.72 [5]. Wang et al. [6] also found that adding carbon fibres to PU/EP (epoxy resin) IPNs increases the $\tan\delta$ from 0.37 to 0.72. One of the weaknesses of polyurethanes is their moderate to low mechanical properties. One of the reasons of this weakness is lack of hydrogen bonding between the hard and soft segments and incompatibility between the polar hard segments and nonpolar soft segments. One proposal to overcome this weakness is to introduce carbon nanoparticles to the neat polyurethane [7].

Graphene is an allotrope of carbon, and with one atom thick planar sheets structure of sp^2 bonded carbon atoms packed in a honeycomb like lattice [8]. Graphene has the intrinsic strength of the monolayer membrane of 42 N m^{-1}, which equates to an intrinsic strength of 130 GPa and Young's modulus of 1 TPa [9]. However, the strength of the interface is central to the mechanical enhancement of graphene modified polymers rather than of the intrinsic strength of graphene particles. Therefore, the functionalised graphene (f-GNP) which form chemical bonding with the matrix is superior to the pristine graphene for mechanical reinforcement of polymers.

The dispersion of graphene in PU makes noticeable contributions to the enhancement of PU mechanical properties [10]. In this regard, surface treating of nanofillers boost the dispersion of the nanopartciles in PU matrices. In addition, the functionalities located on the surface of nanofillers such as hydroxyl, carboxyl, or amine groups can potentially form chemical bonding with PU matrices resulting in a strong interface between the fillers and the matrix for stress transfer.

The f-GNP nanoparticles and polymeric matrices interacts by mechanical interlocking through the wrinkled surface of thin graphene sheets; and chemically by the hydrogen bonding formed between the oxygen functionalities of the f-GNP and polymeric matrices. It was found hydrogen and covalent bondings are formed between graphite oxide nanoplatelets (GONPs) and PUs which act as a strong interface [11]. It is reported that Young's modulus and hardness of a PU with 4.4 wt% GONPs was nearly increased by ~900% and ~327%, respectively, relative to the neat PU due to the covalent interface with the hard segment of the PU [12].

Pokharel et al. manufactured polyurethane (PU) nanocomposites by in-situ polymerization using pristine graphene nanoplatelets (GNPs), graphene oxide (GO), and functionalised graphene sheets (FGSs). Tensile testing, dynamic mechanical thermal analysis and the efficacy of functional groups on the graphene were evaluated for the three PU nanocomposites. The PU nanocomposites modified by 2 wt% loading of GO or FGS showed significantly higher Young's modulus than that the one modified by GNPs [13]. It is reported the detailed structure of the PU, in terms of the composition and specific chemistry of the hard and soft segments, is probably important for the graphene stabilisation and mechanical properties of the resultant graphene/PU composites [14].

The motivation of this research is based on development of a polymer coating for protection of leading edge erosion (LEE) of wind turbine blades. Wave propagation is the main cause of LEE of blades from the impact of rain droplet. The droplet impact causes microcracks which leads to crack formation, crack propagation, spalling, abrasion, and fatigue [15]. The LEE can be prevented and/or delayed by increasing damping properties of blade coatings to absorb and attenuate stress waves and by increasing toughness of the coating for delaying crack initiation and growth. In this study, carbon nanoparticles in the form of functionalised graphene nanoplatelet (f-GNP) alone and in combination with hydrophobic silica-based solution (SG) have been added to neat polyurethane to improve the damping coefficient, toughness and energy absorption of the resultant nanocomposites for coating application in protecting the leading-edge of wind turbine blades.

2. Materials

The two component polyurethanes system BAYTEC® 9005 60A MF Polyol with viscosity of 800–1600 mPa s and specific gravity of 1.01–1.04 and the DESMODUR® B9 M10 polyisocyanates crosslinkers with viscosity of 120–200 mPa s and specific gravity of 1.21–1.23 were supplied by Covestro. The mixing ratio by weight of polyol to hardener is 100:37 and it cures at room temperature. The PU has a tensile strength of 5 MPa, elongation of 198% and resilience of 33%.

The as received functional graphene nanoplatelets material HDPlas™ GNP–COOH having carboxyl groups at their surfaces by a "split plasma" treatment in oxygen by the manufacturer. The plasma functionalisation is a low temperature, low energy, dry process, with no effluent disposal, and is benign to the structure of the raw material. The functional groups were only attached to the edges, dislocation sites and defects. The average lateral dimensions is between 0.3 and 5 μm and typical f-GNP thickness of <0.5 nm, bulk density of 215 kg/m^3 and specific surface area of ~25 m^2/g. The individual graphene sheets are approximately 0.335 nm thick with an aspect ratio of ~85 [16].

Hydrophobic silica-based sol-gel P029™ was supplied by Sol-Gel Materials & Applications (SGAM), Gillingham, UK and contains 15% Si.

Cylindrical rods with 30 mm diameter of polyethylene terephthalate (PET), polytetrafluoroethylene (PTFE), ultra-high molecular weight polyethylene (UHMWPE), PVC, high-density polyethylene (HDPE), and NYLON were purchased from Direct Plastics Limited UK.

3. Manufacture of damping-test specimens

3.1. Material selection

For these experiments, in addition to manufacturing neat polyurethane (PU), graphene modified PU (PU + f-GNP) and graphene/sol-gel modified PU (PU + f-GNP + SG), other ready-made selected PTFE, HDPE, UHMWPE, PET, PVC and NYLON polymers were tested in order in to make comparison. The material characteristics that were considered for analysis are $\tan\delta$ and attenuation. Mechanical loss coefficient ($\tan\delta$), is a factor which shows the effectiveness of a material's damping capabilities. The higher the mechanical loss coefficient, the greater the damping coefficient, hence, material will effectively accomplishing energy absorption and dispersal. Attenuation is the decay rate of the wave as it propagates through the material.

3.2. Test specimen preparation

Specimens of neat polyurethane, graphene modified PU, and f-GNP+SG modified PU were prepared according to the procedures below.

PU specimens: BAYTEC® 9005 60A MF polyol (100 g) was mixed with DESMODUR® B9 M10 polyisocyanates (37 g) at room temperature (25 °C) for 3 min using a homogeniser at 8000 rpm. The mixture was then placed into a degassing chamber for 5 min, poured into a mould and left for 12 h to be cured at room temperature. The mould was made of polyethylene which possesses self-releasing characteristics.

PU + f-GNP specimens: Polyurethane/graphene composites can be prepared by blending or in-situ polymerization approaches. In this work the in-situ polymerization of PU/f-GNPs was carried out by directly mixing GNP–COOH (0.5 wt%) with polyol (100 g) at room temperature (25 °C) and mixed using a homogeniser at 8000 rpm for 18 min, subsequently DESMODUR® B9 M10 polyisocyanates (37 g) was added to the mixture and stirred for 1 min and poured into the mould. The functionalised graphenes act as chemical crosslinkers in PUs.

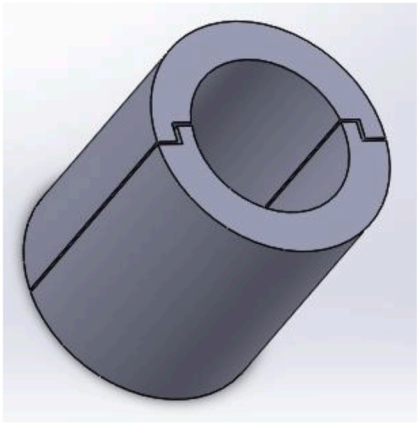

Fig. 1. Using solid works to design a mould from two symmetric pieces.

PU + f-GNP + SG specimens: The in-situ polymerization of PU/f-GNPs was carried out by directly mixing hydrophobic silica-based solution (1 wt%) with the DESMODUR® B9 M10 polyisocyanates (44 g) and then the mixture was added to the mixture of PU + f-GNP (same preparation method as above), stirred for 1 min using a homogeniser at 8000 rpm and poured into the mould.

A cylindrical mould was machined from polyethylene for casting the specimens. There were two options to get the cured samples out of the mould without applying too much stress on them. One method was to manufacture the mould from two symmetric pieces and then bound them together (Fig. 1). The other method was using a milling machine to cut the mould into two pieces and get the samples out of the mould (Fig. 2c). To get the cured specimens out of the mould, at least two layers of mould release agent were applied on the inner surface of the mould before pouring the materials into it. The first layer of the agent was applied by using paint brush and dried for 1 h before the second layer was applied (if it was the first time that the mould is being used for making samples, 6 to 7 layers of release agent needed to be applied). Since the polymer hardens quickly, the process of manufacturing the samples needed to be completed within 7 min. Fig. 2 shows various stages of manufacturing the polyethylene mould and the specimens.

NYLON, HDPE, PTFE, UHMWPE PET and PVC were purchased in 30 mm diameter rods, cut and sanded into 50 mm height specimens. A

Table 1
Specimen's properties for damping test.

Material	Height (mm)	Diameter (mm)
PU	50.2	31.8
PU + f-GNP	49.8	31.9
PU + f-GNP + SG	49.8	32
NYLON	49.8	32
UHMWPE	50.1	31.9
HDPE	49.8	31.8
PTFE	49.9	31.9
PET	49.9	31.7
PVC	50.1	32

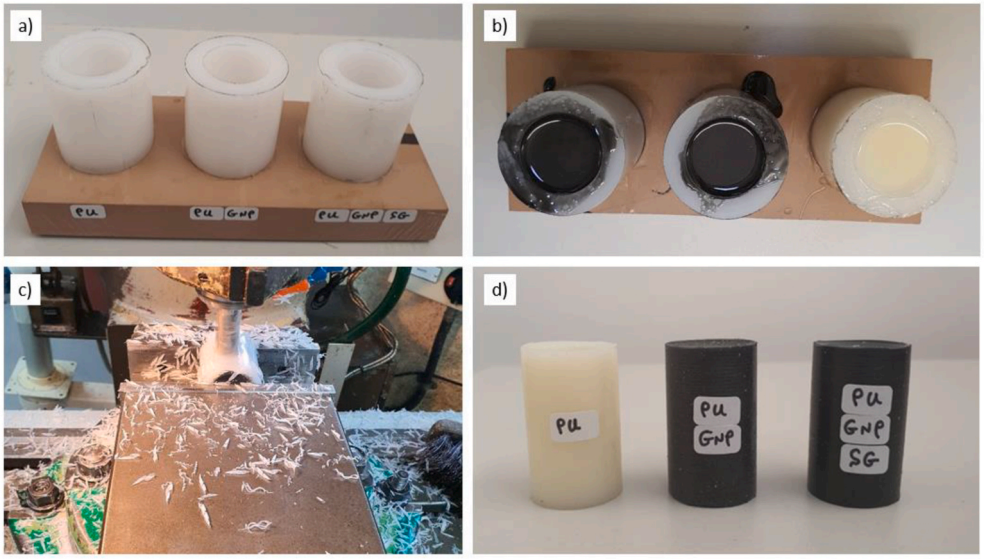

Fig. 2. a) Manufactured mould for making specimens for drop ball test, b) pouring materials into the mould, c) using a milling machine for demoulding specimens, d) final specimens for testing.

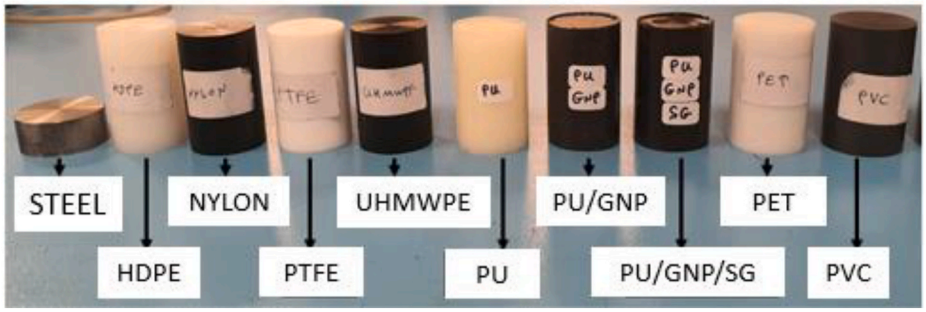

Fig. 3. Specimens for damping test.

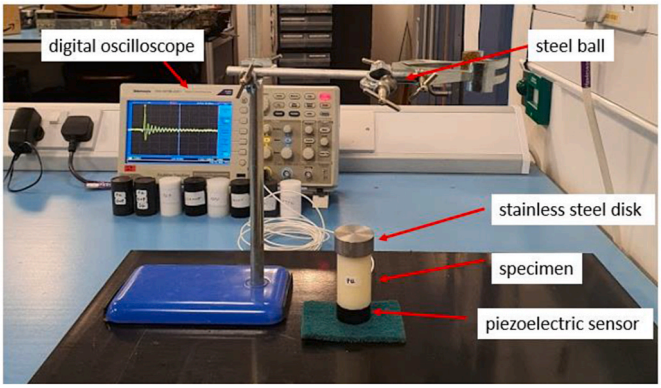

Fig. 4. Damping test set up.

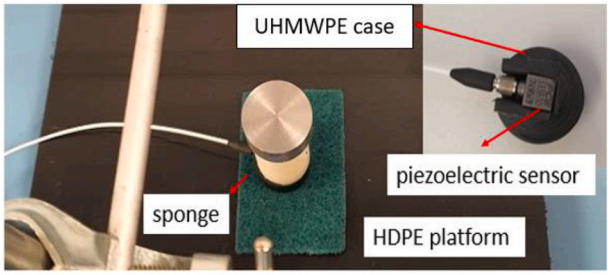

Fig. 5. Piezoelectric sensor set up for the damping test.

stainless steel disk with thickness of 15 mm was made and placed on top of each specimen as the target for the ball drop. The surface condition of the specimens has significant effect on the drop ball test results and the contact surface of the specimens should be very smooth, flat and parallel. To achieve a perfectly smooth surface, 600 grit sand paper was used to sand all specimens. All the specimens that were tested are shown in Fig. 3 and their dimensions are summarised in Table 1.

3.3. Experiment set up

To eliminate the surface hardness effect of the test specimen, the ball was dropped onto the 15 mm thick stainless steel disk, placed on the top of the specimen. A chrome steel ball with 3 mm diameter and hardness of HRC 60–67 was used to generate acoustic signals. The stainless steel disk has hardness up to HRC 40–48. This material is chosen as the target because of its high hardness, thus the steel ball will leave little to no dent on its surface.

As can be seen in Fig. 4, a digital oscilloscope, a piezoelectric sensor, a steel support stand with a screw release clamp and a 3 mm diameter steel ball were used to set up the drop ball test. The piezoelectric sensor was placed under the specimen and aligned vertically facing the bottom face of test specimen. The piezoelectric sensor used here is the PCB 333B30 SNLW56739 made by PCB Piezotronics U.S. which is inserted in a UHMWPE casing and laid on a sponge over an HDPE platform (Fig. 5). The effect of the system vibration is reduced by locating the sensor on a sponge. The acoustic signal is generated by dropping the steel ball onto the target. This signal travels through the test specimen and the reduced outcome signal is received by the piezoelectric sensor which is located at the bottom of the specimen and displayed on a digital oscilloscope. The oscilloscope used here is a TBS-1072-EDU digital oscilloscope made by Tektronix. As can be seen in Fig. 5, the whole system is placed on an HDPE platform to make the setup flat and horizontal and also to prevent the steel ball from hitting the floor after bouncing back.

The impedance mismatch between air and solid materials is large and almost no transmission of ultrasonic waves between the two will happens. For making proper transmission of the ultrasonic signal between the specimen and the ultrasonic sensor, the air gap between them and also between the specimen and stainless-steel target disk were filled with a couplant.

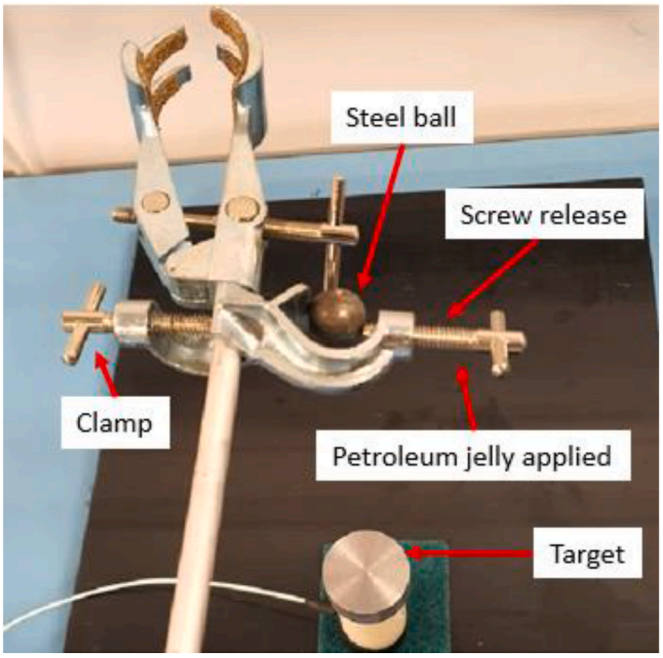

Fig. 6. Holding the steel ball on the rod with a clamp.

The choice of the right couplant materials was based on signal transmission capability, the interaction with test specimen along with consistency and the ease of application during repeated testing. Different couplant materials have different acoustic impedance properties and viscosities which needed to be considered in choosing the right couplant for the test. For this test two types of couplant were initially chosen: petroleum jelly and silicon lubricant. Using petroleum jelly has some disadvantages, for example it was difficult to have a consistent layer thickness for all tests and the different amount of couplant applied each time has a significant effect on the results. Silicon lubricant couplant was ultimately chosen because it is very consistent in application. This couplant will leave trace of a thin layer on the surface of specimen which is not too slippery and allow the steel target to seat on the specimen without sliding off.

To improve the consistency of the test, the residue couplant on the specimen and sensor were wiped off and reapplied in the same way after each drop test.

As can be seen in Fig. 6, the steel ball is held 12 cm above the target with a clamp. The ball is dropped by rotating the screw. To ensure consistency of the test, it is important that each time the ball falls on the centre of the target. For that reason petroleum jelly was applied on the screw to reduce friction. The steel drop-ball is relatively small and so turning the screw should be done gently.

4. Results of the damping tests

To ensure that the results of damping test are reliable, the following points were taking into account during manufacturing of the specimens.

- All specimens were made with the same dimensions, as can be seen in Table 1, height of all specimens is in the range of 49.8–50.2 mm and the diameter of all specimens are between 31.7 and 32.1 mm.
- Surfaces of all the specimens were smooth and parallel to ensure good signal transmission.

Table 2
Test setup of the drop ball test.

Oscilloscope display	5 mv/div; 10 ms/div
Ball size	3 mm
Drop height	12 cm

Table 3
Maximum voltage (mV) for the drop ball test.

Specimen	Maximum Voltage (mV)					
	Test 1	Test 2	Test 3	Test 4	Test 5	Mean with 95% confidence level (v)
PU	17.2	17.2	17.4	17.2	17	17.2 ± 0.1
PU + f-GNP	16.8	16.8	16.6	16.6	16.2	16.6 ± 0.2
PU + f-GNP + SG	17.2	16.8	16.8	17	16.6	16.9 ± 0.2
PTFE	22	20.2	22.6	20.2	20.4	21.1 ± 1.2
PVC	21.2	21	20.6	22.2	20.0	21.0 ± 0.6
NYLON	19.6	19.2	19.8	19.4	19.4	19.5 ± 0.2
HDPE	18.8	18.8	18.4	18.2	18.4	18.5 ± 0.2
UHMWPE	17.8	17.8	17.6	17.4	17.6	17.6 ± 0.1
PET	17.2	17.4	17.6	17.2	17.6	17.4 ± 0.2

The specimens tested were neat polyurethane (PU), graphene modified PU (PU + f-GNP), graphene and hydrophobic silica-based solution modified PU (PU + f-GNP + SG), polytetrafluoroethylene (PTFE), high-density polyethylene (HDPE), ultra-high molecular weight polyethylene fibre (UHMWPE), polyethylene terephthalate (PET), PVC and NYLON. For each specimen, the drop-ball test was repeated 5 times from a drop height of 12 cm above the steel target disc. The maximum voltage of the signal received by the sensor located underneath the specimen was recorded. The lower the voltage, the more the impact signal was attenuated, which indicated a better attenuation capability of the test material. Table 2 shows the test setup specification and Table 3 shows the voltage recorded by the sensor for each drop ball test.

Samples of screen shots of the oscilloscope for each specimen are shown in Fig. 7. It can be seen that different materials responded in very different ways to the drop ball impact, generating different wave signals. Studies show that other factors such as the geometry of the specimen, material properties, type of the coupling and test set up also affects the generated wave signals for different materials [2,3]. Longitudinal wave is generated when a force is applied rapidly normal to a surface. This wave will travel through the material. Particles in the vicinity of the wave move parallel to the direction of wave propagation. As a wave propagate through a medium, its intensity decreases, and as the wave travels its intensity will reduce with distance travelled. Since the dropping of the steel ball is consistent for each test, a higher voltage signal indicates less vibration attenuation, and hence a poorer attenuation capability. It can be seen from Table 3 that PTFE shows the highest voltage as a result of drop ball test and GNP–COOH modified polyurethane (PU + f-GNP) shows the lowest voltage, indicating that graphene modified polyurethane has the highest attenuation. Table 3, shows that this drop ball test set up is able to generate consistent results which produce waves with less than 1% variation in signal strength.

In conclusion, among the PU, PU + f-GNP and PU + f-GNP + SG materials tested in this study, neat polyurethane (PU) has the lowest attenuation (Fig. 8), and this is improved by 3.5% by adding 0.5 wt% of GNP – COOH.

5. Identification of modal parameters with the SVD-QR method

The objective of the drop ball test is to identify the attenuation properties of the various materials. In order to do this, the modal parameters (frequency and damping ratio) of the main deformation modes of the system (those with highest amplitude and lowest frequency) should be identified. This identification is made by analysing the free response of the system after the drop ball impact. Considering linearity and disregarding higher modes (not relevant for the analysis), this free response is a linear combination of exponentially attenuated harmonic signals as shown in equation (2). Each of these signals corresponds to a particular deformation mode of the system and has a characteristic frequency and damping ratio.

The SVD-QR method has been used to do this identification. However, since only one sensor is used during the test, the association between modal parameters and deformation modes is not possible.

The experimental modal analysis (EMA) method employed for the signal analysis was the QR Factorization and Singular Value Decomposition (SVD-QR) method [17,18]. This time-domain method was developed to extract the modal parameters of structural signals of combat aircraft during flutter flight testing carried out at CLAEX (the Spanish Military Flight Test Center). These signals were short, noisy and with close modes, all of which make its analysis difficult.

This method, like most EMA methods, assumes a linear system with viscous damping (proportional to the velocity and opposing motion). It is presumed that the material deformation is elastic and consequently the non-linear effects are negligible. Consequently, the free response of the system can be represented by the following matrix differential equation:

$$[M]\{\ddot{y}\} + [C]\{\dot{y}\} + [K]\{y\} = 0 \tag{1}$$

where M, C, and K represent the matrices of mass, damping, and stiffness respectively and $\{y(t)\}$ is the deformation vector [19].

Therefore, $y(t)$, the deformation in one point of the system, can be represented as exponentially damped harmonic functions:

$$y(t) = \sum_{i=1}^{n} h_i(t) = \sum_{i=1}^{n} \left\{ A_i \sin(2\pi f_i t) e^{-2\pi\xi_i f_i t} + B_i \cos(2\pi f_i t) e^{-2\pi\xi_i f_i t} \right\} \tag{2}$$

This equation indicates that the deformation in one point of the system is the result of the addition of n different modes $h_i(t)$ with the associated frequencies f_i and damping ratio ξ_i (Fig. 9).

The traditional EMA methods try to adjust (e.g. least squares) the experimental values of the response to equation (2) in order to find the 4 values of A_i, B_i, f_i and ξ_i for each of the n modes M_i.

The SVD-QR method takes advantage of a property of linearity of the exponentially damped harmonic functions and consequently of $y(t)$. Assuming that there are n modes and $2n + 1$ periods of time of the same length are taken, the response in one period is a linear combination of the responses in the other $2n$ periods.

Assuming that $2p$ samples of the response $y(t)$ has been acquired, $y(t_1), y(t_2), \ldots, y(t_{2p})$, a Henkel matrix can be built up:

$$H = \begin{pmatrix} y(t_1) & y(t_2) & \cdots & y(t_p) \\ y(t_2) & y(t_3) & \cdots & y(t_{p+1}) \\ \vdots & \vdots & \ddots & \vdots \\ y(t_p) & y(t_{p+1}) & \cdots & y(t_{2p}) \end{pmatrix} \tag{3}$$

Due to the linearity property of $y(t)$ only $2n$ files (or $2n$ columns) are independent, i.e. only $2n$ files are required to represent the whole signal $y(t)$.

As only $2n$ files are necessary, the following step is to select these files and to truncate the matrix H. However, it is paramount to choose the $2n$ files that provide maximum information, i.e. the $2n$ files that are most orthogonal among each other should be selected.

The QR decomposition of the matrix H into a product of an orthogonal matrix Q and an upper triangular matrix R provides a permutation matrix M_p, such that:

$$H \times M_P = Q \times R; \quad Q^T \times Q = I; \quad r_{ij} = 0 \; \forall i > j \tag{4}$$

$$B = M_p^T \times H \tag{5}$$

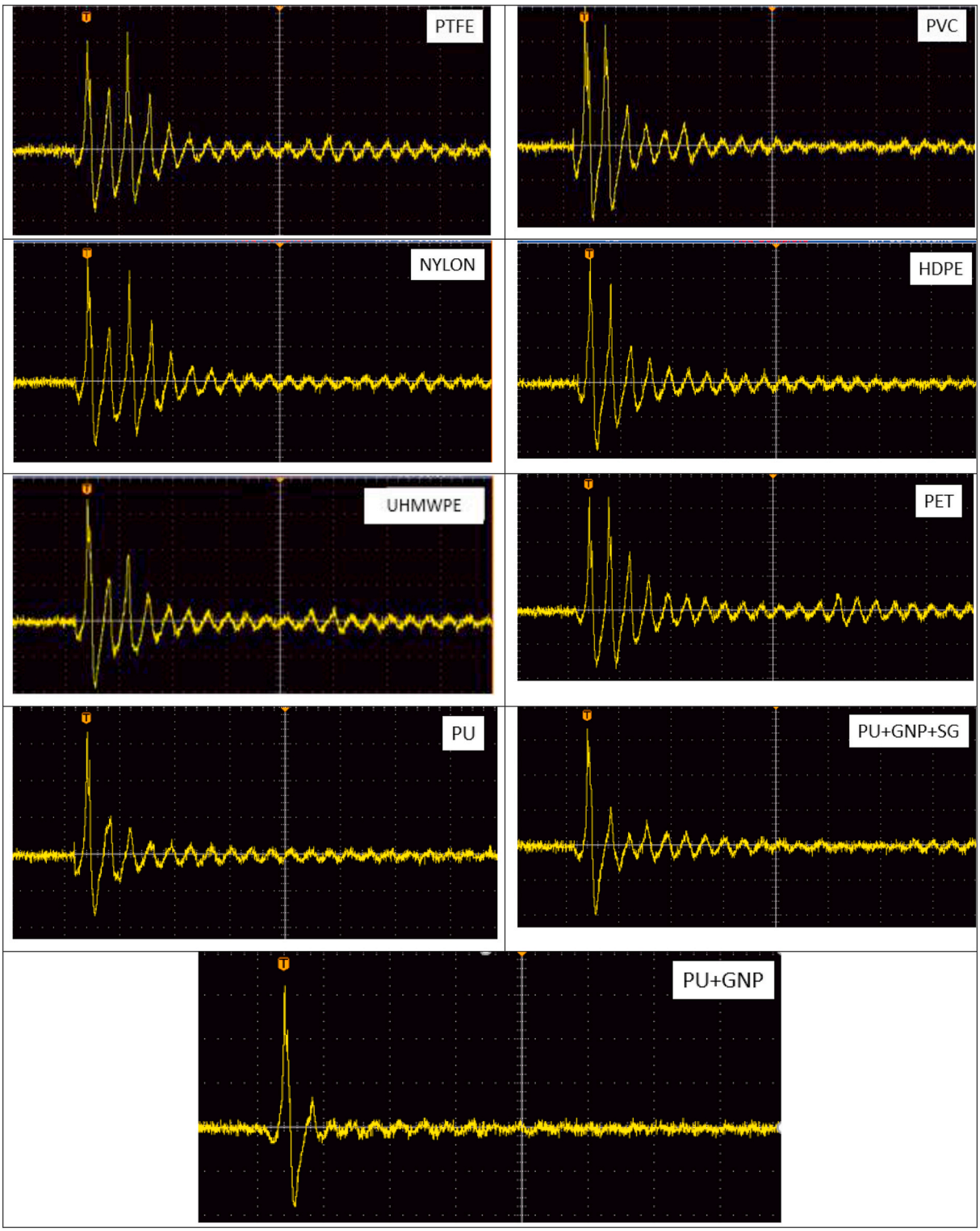

Fig. 7. Wave signals for different specimen as a result of drop ball test.

The files of the matrix H have been reorganised with the permutation matrix M_p in such a way that the $2n$ first files of matrix B provide the maximum of information.

Truncating the matrix B and retaining only the first $2n$ files, the matrix B_t is generated:

$$B_t = \begin{pmatrix} y(t_{s1}) & y(t_{s2}) & \cdots & y(t_{sp}) \\ y(t_{u1}) & y(t_{u2}) & \cdots & y(t_{up}) \\ \vdots & \vdots & \ddots & \vdots \\ y(t_{o1}) & y(t_{o2}) & \cdots & y(t_{op}) \end{pmatrix} \tag{6}$$

Since the function of the response $y(t)$ is well known (Eq. (2)), selecting a frequency f_s and damping ratio ξ_s, a synthetic response can be generated:

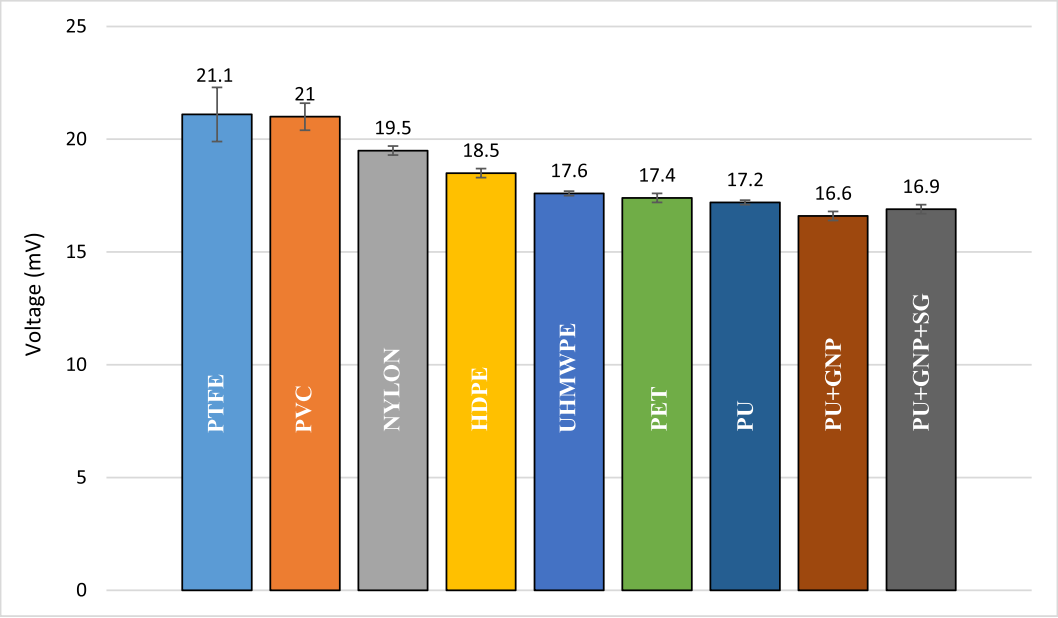

Fig. 8. Highest voltage recorded by oscilloscope for different specimens as a results of drop ball tests.

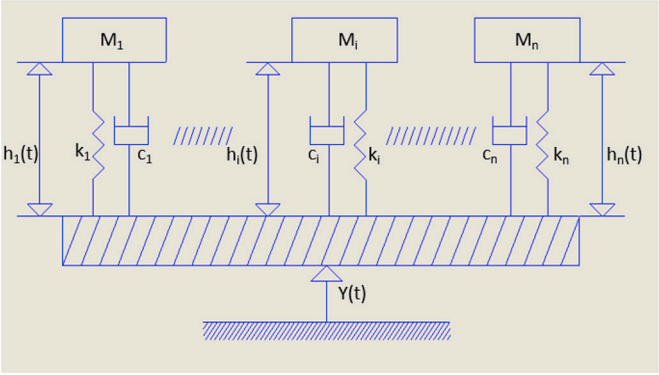

Fig. 9. Equivalent system.

$$x(t_K) = \sin(2\pi f_s t_K) e^{-2\pi\xi_s f_s t_K} \Leftrightarrow X = [\,x(t_1) \quad x(t_2) \quad \dots \quad x(t_p)\,] \Leftrightarrow X^I = \frac{X}{X} \tag{7}$$

The last operation shown in Eq. (6) is the division of the components of vector X by its own Euclidean norm, in such a way the norm of vector X^I is one.

Including the vector X^I in the matrix B_t, the extended matrix B_{te} is created:

$$B_{te}\begin{pmatrix} f_s, \xi_s \end{pmatrix} = \begin{pmatrix} y(t_{s1}) & y(t_{s2}) & \dots & y(t_{sp}) \\ y(t_{u1}) & y(t_{u2}) & \dots & y(t_{up}) \\ \vdots & \vdots & \ddots & \vdots \\ y(t_{o1}) & y(t_{o2}) & \dots & y(t_{op}) \\ x^I(t_1) & x^I(t_2) & \dots & x^I(t_p) \end{pmatrix} \tag{8}$$

In the case, in which, the frequency f_s and the damping ratio ξ_s correspond to a mode $h_i(t)$ of the response, the matrix B_{te} will have a rank very close to $2n$. It cannot be exactly $2n$ because the signal $y(t)$ has always some noise. If the parameters do not correspond to those of a mode the rank would be $2n + 1$.

To assess how close to $2n$ or to $2n + 1$ the rank of the matrix B_{te} is, its pseudo-determinant $\psi(f_s, \xi_s)$ is calculated:

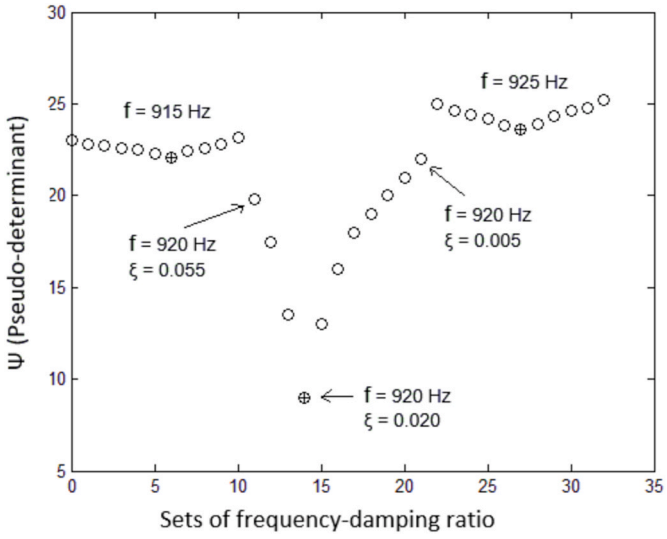

Fig. 10. Pseudo-determinant for values of frequency and damping ratio.

$$B_{te}(f_s, \xi_s) = U \times S \times V^T \Rightarrow S(f_s, \xi_s) = \begin{pmatrix} s_1 & 0 & \dots & 0 \\ 0 & s_2 & \dots & 0 \\ \vdots & \vdots & \ddots & \vdots \\ 0 & 0 & \dots & s_{n+1} \end{pmatrix}; s_1 \geq s_2 \geq \dots \geq s_{n+1} \tag{9}$$

$$\Psi(f_s, \xi_s) = s_1 \times s_2 \times \dots \times s_{n+1} \tag{10}$$

If the ranges of possible values for the modal frequencies and damping ratio of the signal $y(t)$ are known, a search can be performed in such both ranges. In Fig. 10 the range of search for frequency is 915 Hz, 920 Hz and 925 Hz, and the range for damping ratio is from 0.005 to 0.055 with increments of 0.005. In total, as shown in Fig. 10, there are 35 sets of frequency and damping ratio.

For each value in the range of frequencies, the pseudo-determinant was calculated for the combinations of such a value with all possible values of damping ratio. For such a value of frequency, the damping ratio corresponding to the minimum values of pseudo-determinant is chosen. In Fig. 10, for a frequency of 920 Hz, the associated damping

Table 4
Damping coefficient and damping ratio measured by the drop ball test.

Sample	Frequency (200–300 Hz)<		Frequency (500–600 Hz)<		Frequency (700–1000 Hz)<	
	Damping coefficient (**tan δ**)	damping ratio (**ξ**)	Damping coefficient (**tan δ**)	damping ratio (**ξ**)	Damping coefficient (**tan δ**)	damping ratio (**ξ**)
PU	0.0250 ± 0.0017	0.0125	0.0485 ± 0.0073	0.0243	0.0813 ± 0.0041	0.0407
PU+f-GNP	0.0343 ± 0.0061	0.0172	0.0651 ± 0.0012	0.0326	0.1073 ± 0.0044	0.0535
PU+f-GNP+SG	0.0305 ± 0.0026	0.0153	0.0622 ± 0.0079	0.0311	0.0848 ± 0.0023	0.0424
PTFE	0.0210 ± 0.0045	0.0105	0.0290 ± 0.0039	0.0145	0.0348 ± 0.0032	0.0174
PVC	0.0245 ± 0.0035	0.0123	0.0425 ± 0.0079	0.0213	0.0345 ± 0.0016	0.0173
NYLON	0.0240 ± 0.0028	0.0120	0.0525 ± 0.0061	0.0253	0.0350 ± 0.0022	0.0175
HDPE	0.0235 ± 0.0038	0.0117	0.0505 ± 0.0084	0.0253	0.0388 ± 0.0061	0.0194
PET	0.0240 ± 0.0037	0.0120	0.0408 ± 0.0121	0.0204	0.0405 ± 0.0081	0.0203
UHMWPE	0.0245 ± 0.0008	0.0123	0.0415 ± 0.0132	0.0208	0.0435 ± 0.0029	0.0218

ratio is 0.020.

In case the set of frequency and damping ratio, providing minimum pseudo-determinant, corresponded to a mode and the signal $y(t)$ were noiseless, the pseudo-determinant would be zero.

Now, a function associating the frequencies in the searching range with a value of pseudo-determinant (and a value of damping ratio) has been generated.

The minimums of this function correspond to frequencies (and associated damping ratio) of the modes of the response $y(t)$.

When the number of modes of the response is unknown (n is not available). It is useful to calculate the parameters for various values of number of modes and compare the results.

On the other hand, special attention has to be taken when choosing the segment of signal to be analysed. It is important to ensure that it corresponds to a free response and it is not polluted with contributions corresponding to the impact period.

6. Experimental results of damping coefficient using SVD-QR method

There are three different types of damping: coulomb damping caused by kinetic friction between sliding dry surfaces; viscous damping which happens when heat is dissipated due to the movement of bodies in a liquid medium; and the third type is hysteresis damping: when a solid is deformed and heat is dissipated by internal friction. Hard materials such as metals and ceramics do not show hysteresis damping under a moderate load but soft materials like polymers exhibit large hysteresis damping [20]. Damping capability is influenced by different factors such as the nature of material, modulus, frequency, temperature and defects [20].

For shock absorption, vibration control, and noise reduction, materials with high damping coefficients are required. Viscoelastic properties and glass transition temperature are two important factors which influence the vibration damping of polymers [20]. Polyurethanes are attractive for damping applications as they can be modified in order to change their glass transition temperature [21,22]. PU with strong degree of microphase separation present superior mechanical property as each pure phase possess the best required properties, e.g. low T_g of the soft segment chains, and high melting temperature (T_m) of hard segment chains which gives high heat resistance, Young's modulus and tensile strength. In fact, controls of hard segment content and chemical cross-linking density controls the mechanical properties of Pus [23].

The addition of carbon nanoparticles to PU can affect the T_g in two different ways: it can increase the T_g by restricting the molecular motion due to the well-dispersed carbon nanoparticles; or can reduce the T_g by modifying the degree of phase separation (DPS) [24,25]. It is known that in a polyurethane structure there are two different types of carbonyl groups (C=O), some of them are located at the interfacial zone between hard and soft segments which can be either free or H-bonded and some of them are located in the hard domain which are H-bounded only. DPS or degree of hard segment linking hard segments can be calculated using the equation:

$$\mathrm{DPS} = \frac{Cb_{C=O}}{Cf_{C=O} + Cb_{C=O}} \tag{11}$$

Where C_b is the coefficient of hydrogen bounded urethane and C_f is the free urethane [26].

Comparing PU20 containing 20% hard segment +1 wt% f-GNP with PU40 containing 40% hard segment + 1 wt% f-GNP showed that PU40 has higher $T_g = 46\,^{\circ}C$ than PU20 with $T_g = 41^{\circ}C$ [27]. It should be noted that adding nanomaterials may not increase the glass transition temperature of the PU if the nanomaterials dispersion in the polymeric matrix is poor and not uniform [28].

Damping is the conversion of mechanical energy of a structure into thermal energy. A system is classified according to its damping ratio ξ as: underdamped if $\xi < 1$, critically damped if $\xi = 1$, and overdamped if $\xi > 1$. In all these cases, the response of a system set into motion will eventually decay to zero with time, except when $\xi = 0$ [29].

The damping coefficient tan δ can be calculated from:

$$\tan\delta = 1/n\pi \tag{12}$$

Where n is number of cycles the signal decays. The first order damped system amplitude multiplier is $e^{-\xi\omega_n t}$. So when the exponent is equal to -1, it will have a decay magnitude of e and therefore,

$$\xi = 1/\omega_n t \tag{13}$$

Hence,

$$\tan\delta = 2\xi = \frac{2}{\omega_n t} \tag{14}$$

Polyurethanes are classified as underdamped materials and their damping ratio typically range from 0.05 to 0.15 [30–33], e.g. damping coefficient of the PU at 30 °C is reported 0.1 [32] and at room temperature and 1000 Hz is 0.05 [33]. Experimental results of damping coefficient (tan δ) and damping ratio (ξ) of the drop ball tests with 95% confidence level at specified frequencies are summarised in Table 4.

Fig. 11 shows Pseudo-determinant ψ for different frequency and damping values for all materials tested in this study. The damping coefficient value of each material is in Table 5. Inspection of Table 5 shows that the voltage results decrease as tan δ and attenuation increase which means that when a material has low damping coefficient it has less ability to dissipate the energy of the system and that is why the sensor records higher voltage as a result of drop ball test. Among all materials tested in this study, GNP–COOH modified polyurethane has the highest damping coefficient and shows the lowest voltage recorded by the sensor indicating it is the best attenuating material among tested materials. PTFE and PVC show the highest voltage recorded and the lowest damping coefficients.

Plots of the damping coefficient versus voltage for frequency range 200–300 Hz, 500–700 Hz and 700–1000 Hz are shown in Fig. 12. From this plot it is evident that the PU and graphene modified PU have higher damping coefficient at higher frequencies, and PU +GNP nanocomposite

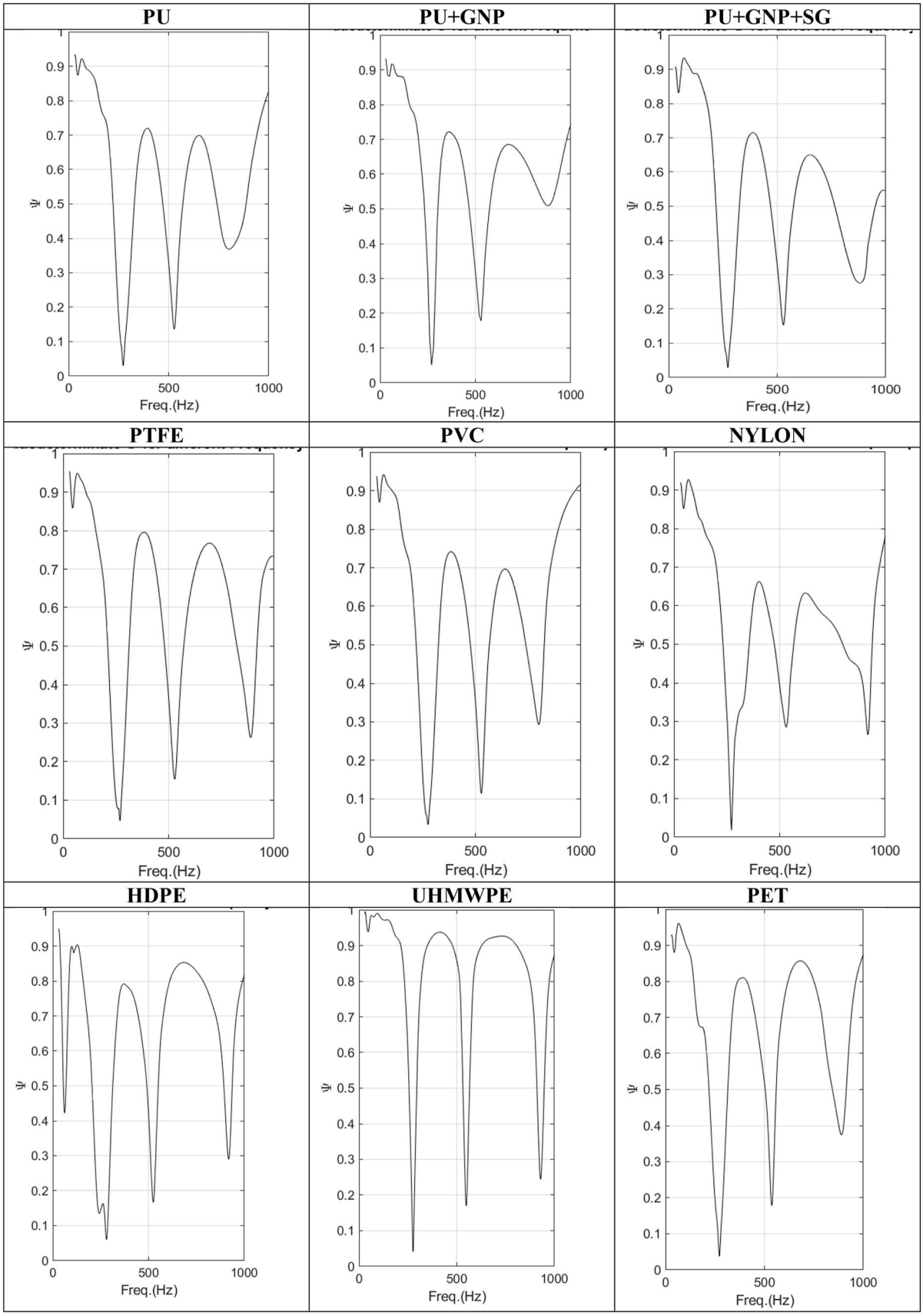

Fig. 11. Drop ball test results analysis by SVD-QR for all tested materials.

Table 5
Sensor maximum voltage, damping coefficient and tan δ for three frequency ranges for all samples.

Material	Voltage (mV)	Frequency (200–300 Hz)<	Frequency (500–600 Hz)<	Frequency (700–1000 Hz)
		tan δ	**tan δ**	**tan δ**
PU	17.2	0.0250 ± 0.0017	0.0485 ± 0.0073	0.0813 ± 0.0041
PU+f-GNP	16.6	0.0343 ± 0.0061	0.0651 ± 0.0012	0.1073 ± 0.0044
PU+f-GNP+SG	16.9	0.0305 ± 0.0026	0.0622 ± 0.0079	0.0848 ± 0.0023
PTFE	21.1	0.0210 ± 0.0045	0.0290 ± 0.0039	0.0348 ± 0.0032
PVC	21	0.0245 ± 0.0035	0.0425 ± 0.0079	0.0345 ± 0.0016
NYLON	19.5	0.0240 ± 0.0028	0.0525 ± 0.0061	0.0350 ± 0.0022
HDPE	18.5	0.0235 ± 0.0038	0.0505 ± 0.0084	0.0388 ± 0.0061
PET	17.4	0.0240 ± 0.0037	0.0408 ± 0.0121	0.0405 ± 0.0081
UHMWPE	17.6	0.0245 ± 0.0008	0.0415 ± 0.0132	0.0435 ± 0.0029

has 3.14 time increase in damping coefficient at 700–1000 Hz relative to its damping coefficient at low frequency range of 200–300 Hz. Among PU and nanomodified PU, the highest damping coefficient at all frequency ranges belongs to PU + GNP nanocomposite. Previous work has shown that the graphene increases the damping coefficient and the tortuosity of the neat polyurethane by decreasing the cell size of the PU structure and simultaneously the high aspect ratio and surface area/volume ratio of graphene contribute to the very efficient "stick-slip mechanism" of vibration damping at PU/GNP interfaces, which cause more energy dissipated by interfacial sliding [34].

Fig. 13 show variation of damping coefficient (tan δ) versus frequency for the PU, PU + GNP and PU + GNP + SG. The trend is that at higher frequencies tan δ will increase for all three type of polyurethanes. Also it can be seen that adding f-GNP to PU has significant effect on the amount of increase in tan δ for all three frequency ranges, but adding GNP + SG to PU had only significant effect on tan δ in frequency range of 200–300 Hz and 500–600 Hz and at high frequency range of 700–1000 Hz its effect is diminishing.

7. Conclusion

In this study the damping properties of f-GNPs and f-GNP/SG based PU nanocomposites together with untreated PU for three different frequency ranges have been investigated by a drop ball test. The damping properties of HDPE, NYLON, PET, PTFE, and UHMWPE were also measured for comparison.

In drop ball test, the amount of voltage recorded by the piezoelectric sensor is very sensitive to the experimental setup, test specimen preparation and surface condition of the specimen. By keeping the experimental condition stable, and also by repeating the test on each specimen five times, reliable results have been obtained. The test results at 95% confidence level show that PTFE and PVC attenuate the least and PU + f-GNP, PU + f-GNP + SG and neat PU attenuate the most. It was shown that graphene modified polyurethane has the highest damping coefficient among all tested materials at all frequency ranges.

The singular value decomposition and QR factorization method has been applied to the analysis of drop ball test data and the frequency and

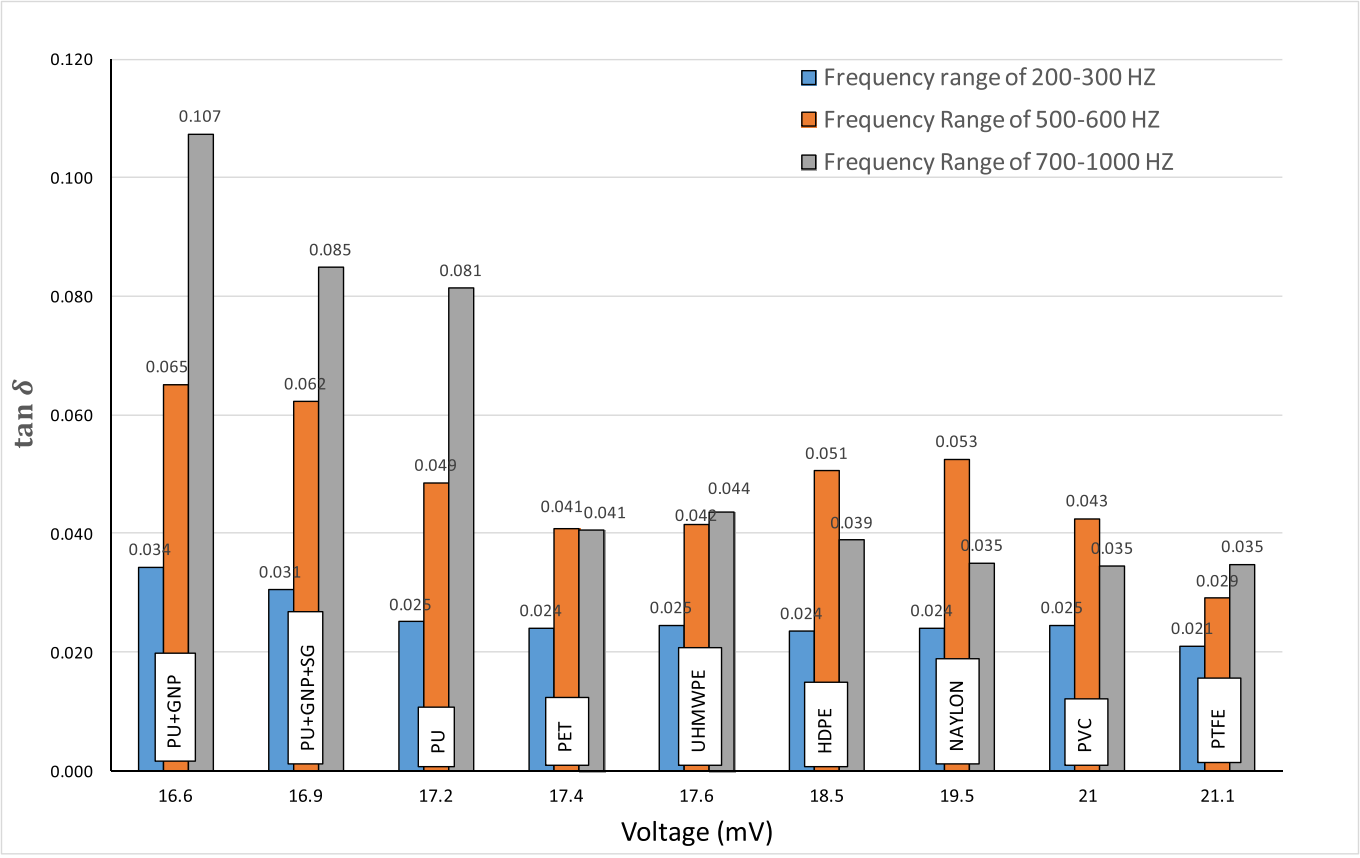

Fig. 12. Damping coefficient vs. maximum voltage in the frequency range of 200–300 Hz, 500–600 Hz and 700–1000 Hz.

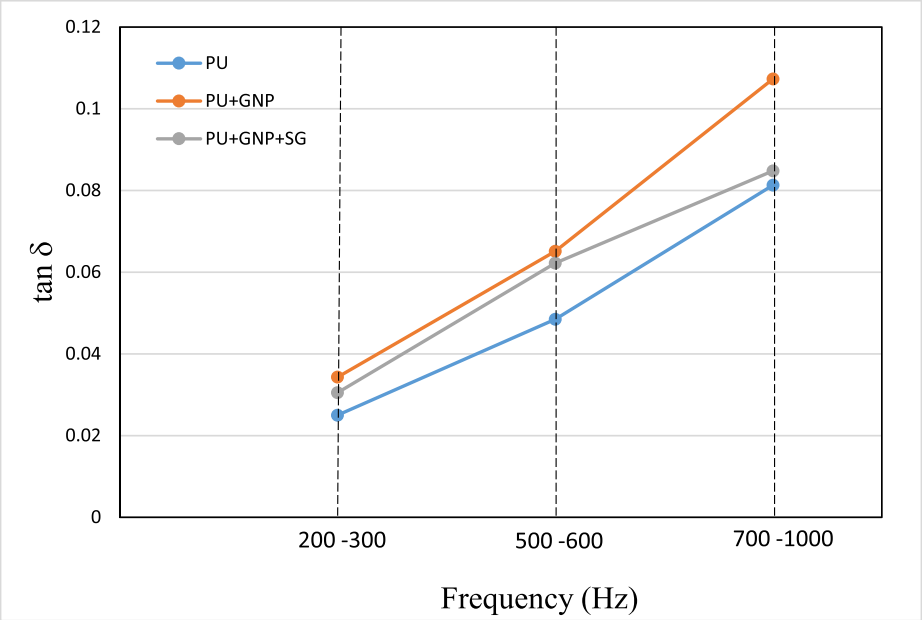

Fig. 13. tan δ at three frequency ranges for PU, PU+GNP and PU+GNP+SG.

damping of the relevant modes are identified. The results show that by adding GNP–COOH (0.5 wt%) to neat polyurethane, the damping coefficient increased by 37.2% for the 200–5300 Hz range, increased by 34% for the 500–600 Hz range and increased by 32% for the 700–1000 Hz range. Adding 1 wt% hydrophobic silica-based solution to the GNP–COOH modified polyurethane increases the damping coefficient of the PU by 22% for the 200–300 Hz range and 28% for the 500–600 Hz range. However, there is no significant effect on the damping coefficient for 700–1000 Hz range.

In summary, the carboxyl functionalised graphene nanoplatelets (GNP–COOH) increases the damping coefficient of the neat polyurethane by decreasing the cell size of the PU structure and simultaneously the high aspect ratio and surface area/volume ratio of graphene contribute in very efficient "stick-slip mechanism" of vibration damping at PU/f-GNP interfaces. The developed polyurethane nanocomposite materials have great potential for protecting leading edge erosion of wind turbine.

Declaration of competing interest

The authors declare that they have no known competing financial interests or personal relationships that could have appeared to influence the work reported in this paper.

References

[1] N. Liu, G. Song, J. Yi, Y. Xu, Damping analysis of polyurethane/polyacrylate interpenetrating polymer network composites filled with graphite particles, Polym. Compos. 34 (2) (2013) 288–292.
[2] Y. Zhang, Measuring Acoustic Attenuation of Polymer Materials Using Drop Ball, Embry-Riddle Aeronautical University, Florida, 2013.
[3] D. Ensminger, L. Bond, Ultrasonics Fundamentals, Technologies, and Applications, CRC Press, 2011.
[4] M. Nakamura, Y. Aoki, G. Enna, K. Oguro, H. Wada, Polyurethane damping material, J. Elastomers Plastics 47 (6) (2014) 515–522.
[5] T. Trakulsujaritchok, D. Hourston, Damping characteristics and mechanical properties of silica filled PUR/PEMA simultaneous interpenetrating polymer networks, Eur. Polym. J. 42 (11) (2006) 2968–2976.
[6] T. Wang, S. Chen, Q. Wang, X. Pei, Damping analysis of polyurethane/epoxy graft interpenetrating polymer network composites filled with short carbon fiber and micro hollow glass bead, Mater. Des. 31 (8) (2010) 3810–3815.
[7] Y. Li, H. Jiao, G. Pan, Q. Wang, T. Wang, Mechanical and damping properties of carbon nanotube-modified polyisobutylene-based polyurethane composites, J. Compos. Mater. 50 (7) (2015) 929–936.
[8] P. Pötschke, A.R. Bhattacharyya, A. Janke, H. Goering, Melt mixing of polycarbonate/multi-wall carbon nanotube composites, Compos. Interfac. 10 (4–5) (2003) 389–404.
[9] C. Lee, X.D. Wei, J.W. Kysar, J. Hone, Measurement of the elastic properties and intrinsic strength of monolayer graphene, Science 321 (5885) (2008) 385–388.
[10] X. Wang, Y. Hu, L. Song, H. Yang, W. Xing, H. Lu, In situ polymerization of graphene nanosheets and polyurethane with enhanced mechanical and thermal properties, J. Mater. Chem. 21 (2011) 4222.
[11] M. Song, D. Cai, Polyurethane nanocomposites by in-situ polymerization approach and their properties, in: In-Situ Synthesis of Polymer Nanocomposites, Wiley, 2011, pp. 169–220.
[12] D. Cai, K. Kamal Yusoh, M. Song, The mechanical properties and morphology of a graphite oxide nanoplatelet/polyurethane composite, Nanotechnology 20 (8) (2009), 085712.
[13] P. Pokharel, B. Pant, K. Pokhrel, H.R. Pant, J.G. Lim, H.Y. Kim, S. Choi, Effects of functional groups on the graphene sheet for improving the thermomechanical properties of polyurethane nanocomposites, Composites Part B 78 (2015) 192–201.
[14] U. Khan, P. May, A. O'Neill, J.N. Coleman, Development of stiff, strong, yet tough composites by the addition of solvent exfoliated graphene to polyurethane, Carbon 48 (14) (2010) 4035–4041.
[15] L. Mishnaevsky Jr., "Toolbox for optimizing anti-erosion protective coatings of wind turbine blades: overview of mechanisms and technical solutions, Wind Energy 22 (11) (2019) 1636–1653.
[16] H.M. Chong, S.J. Hinder, A.C. Taylor, Graphene nanoplatelet-modified epoxy: effect of aspect ratio and surface functionality on mechanical properties and toughening mechanisms, J. Mater. Sci. 51 (2016) 8764–8790.
[17] J. Barros-Rodriguez, R.F. Le Roux, J. Lopez-Diez, R. Martinez-Val, Frequency and damping identification in flutter flight testing using singular value decomposition and QR factorization, Proc IMechE Part G: J. Aero. Eng. 229 (3) (2015) 323–332.
[18] J. Barros-Rodriguez, M.F. Fructuoso, R.F. Le Roux, S.S. Prieto, O.R. Polo, Unveiling modal parameters with forced response using SVD and QR during flutter flight testing, Proc IMechE Part G: J. Aero. Eng. 232 (1) (2018) 68–76.
[19] H. Sönnerlind, Comsol, 14 03, [Online]. Available: https://uk.comsol.com/blogs/damping-in-structural-dynamics-theory-and-sources/, 2019. (Accessed 12 May 2020).
[20] V. Geethamma, R. Asaletha, N. Kalarikkal, S. Thomas, Vibration and sound damping in polymers, Resonance 19 (9) (2014) 821–833.
[21] K. Yoon, J. Kim, D. Bang, Damping properties and transmission loss of polyurethane. II. PU layer and copolymer effect, Fibers Polym. 4 (2) (2003) 49–53.
[22] M. Song, D.J. Hourston, F.U. Schafer, Correlation between mechanical damping and interphase content in interpenetrating polymer networks, J. Appl. Polym. Sci. 81 (10) (2001) 2439–2442.
[23] K. Kojio, S. Nozaki, A. Takahara, S. Yamasaki, Influence of chemical structure of hard segments on physical properties of polyurethane elastomers: a review, J. Polym. Res. 27 (140) (2020).
[24] H. Xia, M. Song, "Preparation and characterization of polyurethane–carbon nanotube composites, Soft Matter 1 (5) (2005) 386.
[25] A. Pei, J. Malho, J. Ruokolainen, Q. Zhou, L. Berglund, Strong nanocomposite reinforcement effects in polyurethane elastomer with low volume fraction of cellulose nanocrystals, Macromolecules 44 (11) (2011) 4422–4427.
[26] M. Bernal, I. Molenberg, S. Estravis, M. Rodriguez-Perez, I. Huynen, M. Lopez-Manchado, R. Verdejo, Comparing the effect of carbon-based nanofillers on the

physical properties of flexible polyurethane foams, J. Mater. Sci. 47 (15) (2012) 5673–5679.
[27] M. Strankowski, Effect of variation of hard segment content and graphene-based nanofiller concentration on morphological, thermal, and mechanical properties of polyurethane nanocomposites, Int. J. Polym. Sci. (2018) 1–20.
[28] J. González-Irún Rodríguez, P. Carreira, A. García-Diez, D. Hui, R. Artiaga, Nanofiller effect on the glass transition of a polyurethane, Therm. Anal. Calorimetr. 87 (1) (2007) 45–47.
[29] P. Macioce, Viscoelastic Damping 101, Sound Vibration 37 (4) (2003) 8–10.
[30] N. Ahmad, A Methodology for Developing High Damping Materials with Application of Noise Reduction of Railway Track, University of Southamppton, 2009.
[31] M. Razmara, S. Saidpour, S. Arunchalam, DMA investigation on polyurethane (PUR), in: International Conference on Fascinating Advancement in Mechanical Engineering, 2008. London.
[32] J. Chang, B. Tian, L. Li, Y. Zheng, Microstructure and damping property of polyurethane composites hybridized with ultraviolet absorbents, Adv. Mater. Sci. Eng. (2018) 1–9.
[33] K. Lee, J. Choi, S. Kim, B. Lee, J. Hwang, B. Lee, Damping and mechanical properties of composite composed of polyurethane matrix and preplaced aggregates, Construct. Build. Mater. 145 (2017) 68–75.
[34] J. Mun Kim, D. Hoon Kim, J. Kim, J. Wook Lee, W. Nyon Kim, Effect of graphene on the sound damping properties of flexible polyurethane foams, Macromol. Res. 25 (2) (2017) 190–196.